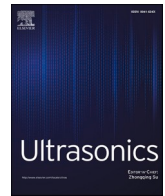# Dispersion of the surface phonons in semiconductor/topological insulator Si/Bi$_2$Te$_3$ heterostructure studied by high resolution

(article starts on next page)

Dispersion of the surface phonons in semiconductor/topological insulator Si/Bi$_2$Te$_3$ heterostructure studied by high resolution Brillouin spectroscopy

A. Trzaskowska [a],[*], S. Mielcarek [a], M. Wiesner [a], F. Lombardi [b], B. Mroz [a]

[a] Faculty of Physics, Adam Mickiewicz University, Uniwersytetu Poznańskiego 2, 61-614 Poznan, Poland
[b] Department of Microtechnology and Nanoscience, Chalmers University of Technology, SE-412 96, Göteborg, Sweden

ABSTRACT

The dynamics and dispersion of surface phonons in heterostructure semiconductor/ topological insulator Si/ Bi$_2$Te$_3$ was investigated using high resolution Brillouin light scattering method in the GHz frequency range. Both Rayleigh and Sezawa surface acoustic waves have been observed for wave vectors ranging from 0.006 to 0.023 nm^{-1}. Anomaly in dispersion relations $\omega(q)$ for both surface waves were detected for the wave vector $q = 0.016$ nm^{-1}. The finite element method (FEM) was used to simulate the observed shapes of $\omega(q)$ and to find the deformation profiles of surface acoustic waves. We attribute the observed changes to the coupling between low energy electrons and surface phonons. The coupling between helical Dirac states and surface phonons is discussed in the frame of accessible theoretical models.

1. Introduction

The search for possible applications of topological insulators (TI) requires knowledge of their physical properties in the form of thin films on various substrates. So, the surface phonon dynamics in heterostructures reported here seems to be an important issue worth learning more about. Understanding the phonon transport properties of thin films is essential for better understanding the electron phonon coupling (EPC) effect [1] or thermal management of micro and nano electronics [2,3].

Spatial limitations of phonons in nanostructures affect their dispersion relation. Additionally, interactions with other phonons, defects and electrons may be changed. On the other hand when the phonon thermal conductivity in nanostructures is considered the boundary scattering is dominant and thermal conductivity scales with the size D [4] as $\kappa \sim C_p v_S \Lambda \sim C_p v_S D$, where C_p is the thermal heat capacity at constant pressure, v_S is the phonon velocity and Λ is average phonon mean free path. Controlling phonon transport by the structure asymmetry or lattice nonlinearity opens new possibilities, such as a practical realization of the thermal diode [5].

Dimensionality reduction can be carried out in two ways: by producing a thin film (for example molecular beam epitaxy) or exfoliating thin flakes (nanosheets) from bulk material. The latter procedure has recently become the subject of intense research, especially in the field of nano-electonics applications [1]. This interest comes from the fact that

after exfoliation van der Waals materials remains strongly bonded two-dimensional (2D) layers that are bound in the third dimension through weaker dispersion forces [6] although automating this process is still an open question.

The acoustic properties of topological insulators thin films have not yet been explored fully so far. In our recent papers [7] it was shown that the electron–phonon interaction at a conducting interface between a topological insulator thin film and a semiconductor substrate can be directly probed by means of high-resolution Brillouin light scattering (BLS). The observation of anomalies in the surface phonon dispersion curves of a thin Bi$_2$Te$_3$ film on GaAs, besides demonstrating important electron–phonon coupling effects in the GHz frequency domain, shows that information on deep interface electrons can be obtained by tuning the penetration depth of surface phonons so as to selectively probe the interface region. Li et al [8] have theoretically investigated the properties of surface acoustic waves (SAW) absorption by TI thin films. They have found that due to momentum and energy conservation laws, the SAW absorption by TI thin films can only be achieved via intra-band electronic transition channel. More interestingly, they found that the absorption of the SAWs by TI thin films can be markedly enhanced by the tunable subgap in the Dirac energy spectrum of the TI surface states.

In a single crystal form Bi$_2$Te$_3$ exhibit a layered rhombohedral lattice structure (space group $R\bar{3}m$) with three quintuple layers (QL) stacks forming a unit cell. Each quintuple layer consists of five atoms with two

---

equivalent Te atoms, two equivalent Bi atoms and a third Te atom [9]. The coupling is strong between two atomic layers within one QL while in two neighboring QLs the coupling is much weaker mainly because of the van der Waals (vdW) bonding [10,11]. Because of the layered structure, the crystals show cleavage plane perpendicular to the [0001] direction.

Bi_2Te_3 is known for many years because of its thermoelectric properties [12-14]. So far elastic properties of single crystals of Bi_2Te_3 have been studied experimentally using the ultrasonic method [15,16] and nanoindentation [17] supported by density functional theory (DFT) [17], local density approximation (LDA) [17] and Perdew-Burke-Ernzerhof (PBE) algorithm [17]. In our recent paper [18] we report on surface phonons dynamic in the single crystal of Bi_2Te_3. Two surface acoustic waves have been observed, which distinguishes this material from other metals or nontransparent materials.

The knowledge of interface electron–phonon interaction has great relevance in the engineering of low-power nanoelectronics as well as in thermoelectric materials such as Bi_2Te_3 and Bi_2Se_3 films epitaxially grown on semiconductors [19].

EPC changes the phononic spectrum of a metal and Kohn anomaly [5,9] can be observed as a discontinuity in the derivative of the dispersion relation that occurs at certain high symmetry points of the first Brillouin zone, produced by the abrupt change in the screening of lattice. Kohn anomalies have been observed mainly in the bulk metallic materials during the different experiments covering the different parts of Brillouin zone: helium atom surface scattering (HASS) was used to study the dispersion relation in topological insulator Bi_2Se_3 [20], inelastic x-ray scattering measurements of the temperature dependence of phonon dispersion in the charge-density-wave (CDW) compound 2H-NbSe$_2$ [21]. Neutron scattering studies revealed the distinct Kohn anomaly in the charge-transfer salt TTF-TCNQ [22], pure Pb [15] or in the one-dimensional conductor $K_2Pt(CN)_4Br_{0.3}$ $3H_2O$ [16].

In this paper we present results of Brillouin spectroscopy of heterostructure: Bi_2Te_3 thin films placed on silicon substrate. The main goal of this study was to investigate whether the dispersion relation measured over the range of phonon energies (few GHz $\approx 10^{-2}$ meV) available in the experiment is sensitive to EPC. We believe the results of high-resolution Brillouin experiments on dynamics and dispersion of energy of surface phonons in heterostructure semiconductor / topological insulator Si/Bi_2Te_3 may give interesting results in the field of phonon engineering.

2. Materials and methods

2.1. The samples

Bi_2Te_3 thin films were grown by MBE on Si (1 1 1), with a 2° off-cut towards [1 1 1]. After eatching in HF and NH_2F solution the samples were quickly loaded into the MBE growth chamber [23]. Then the Si substrate was annealed at 600 °C to remove the surface oxide. Before the growth procedure semiconductor substrates were exposed to Te for 1 min at elevated temperature to passivate the dangling bonds. Bi_2Te_3 growth temperature was 220 °C. The beam equivalent pressures (BEP) of Te and Bi were 10^{-6} Torr and 10^{-8} Torr, respectively resulting in a growth rate of 50 nm/h. First a seed layer was grown at a temperature of 180 °C for 4 min and then the temperature was raised to 220 °C at a rate of 15 °C/min. This procedure was repeated 150 times, resulting in total film thickness of 70 nm. The surface carrier densities measured for Si/Bi_2Te_3 were found to be 1.5 10^{16} cm^{-2}.

2.2. Surface Brillouin spectroscopy

The propagation of surface acoustic waves in TI/Si was studied using a six-pass, tandem Brillouin spectrometer (JRS Scientific Instruments) which ensures a contrast of 10^{15} [24-26]. The source of light used was an Nd:YAG single-mode diode-pumped laser of maximum power 200 mW, emitting the second harmonics of the length $\lambda_0 = 532$ nm (model: Excelsior, manufactured by: Spectra Physics). The incident light was
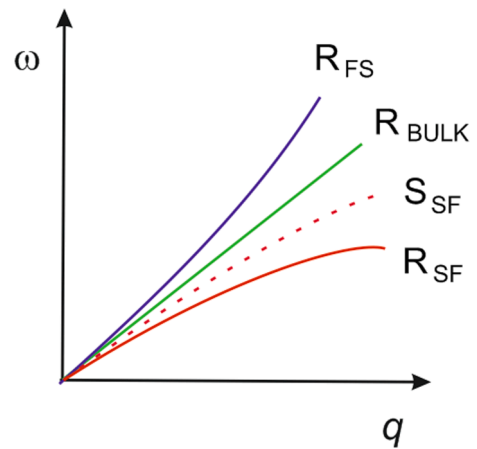
Fig. 1. Dispersion relation of SAW. Red lines Sezawa (S_{SF}) and Rayleigh (R_{SF}) waves in the "slow-on-fast" (SF) case, green line - Rayleigh wave on bulk material, blue line Rayleigh R_{FS} "fast-on-slow" (FS).

polarized in the sagittal plane defined by the wave vector of a given phonon and the normal to the sample surface [24].

Measurements were made in the backscattering geometry. By changing the angle Θ between the incident and normal to the sample surface it is possible to observe the surface phonons with the wave vectors q ranging from 0.006 nm^{-1} to 0.023 nm^{-1} with resolution 0.0002 nm^{-1}. The resolution of frequency is about 0.04 GHz. Both incident and scattered light was polarized vertically.

3. FEM simulations

The calculations of the dispersion relation for the surface phonon propagating in the heterostructure semiconductor/topological insulator were performed using Finite Element Method (FEM), as implemented in the COMSOL Multiphysics software [27]. The periodic boundary conditions that match Floquet conditions had been directly implemented in FEM. The finite element method converts a partial differential equation into a set of linear equations upon interpolating the sought function into locally-defined basis functions (known as finite elements) [28].

The unit cell selected for simulation consisted of a long semiconductor rectangular bar (100 × 100 × 2000 nm^3) loaded with a thin layer (70 nm) of Bi_2Te_3.

4. Results

Brillouin spectroscopy of surface phonons provides information on their dynamics and dispersion in bulk materials and thin films deposited on various substrates. In case of bulk material only Rayleigh can be observed. When studying surface phonons in any heterostructure two cases can be distinguished. The system can be off loaded (slow-on-fast case when velocity of transverse wave propagation in the layer v_T^L is lower than that in the substrate v_T^S) or stiffened (fast-on-slow case, velocity of transverse wave propagation in the layer v_T^L is greater than that in the substrate v_T^S). Fig. 1 presents the different types of dispersion relations $\omega(q)$ of surface phonons accessible in the Brillouin scattering experiments.

According to Farnell and Adler [29], the main criterion of the above classification is $v_T^L < \sqrt{2}v_T^S$ for slow-on-fast systems and $v_T^L > \sqrt{2}v_T^S$ for fast-on-slow ones. For slow-on-fast systems the presence of an elastically soft layer on an elastically hard substrate leads to a reduction of the Rayleigh surface acoustic waves and formation of higher - order modes known as Sezawa waves. The both modes are expected to appear in the spectrum showing a nonlinear dispersion. Both the velocity of surface acoustic waves v_{SAW} and phonon wave vector q depend on angle Θ between scattered light and normal to sample plane as follows:
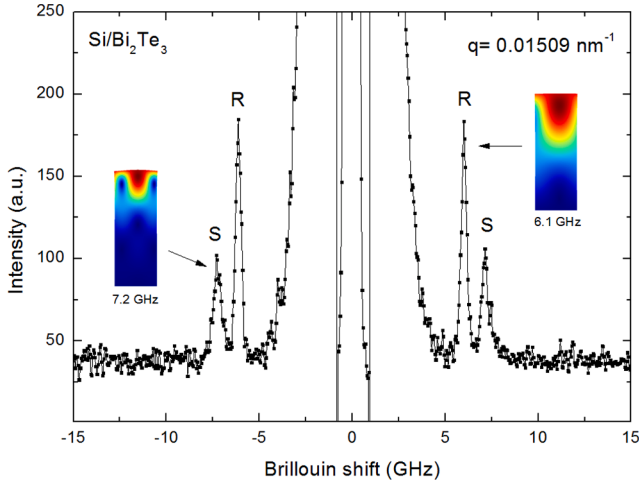
Fig. 2. Typical surface Brillouin spectrum of Si/Bi$_2$Te$_3$ heterostructure showing two modes: Sezawa (S) and Rayleigh (R). Accumulation time was about 120 min (12000 sweeps), laser power on the sample was reduced to 90 mW. The thickness of Bi$_2$Te$_3$ film was 70 nm. Color insets: total displacement profile showing acoustic wave mode shapes (R - Rayleigh wave, S - Sezawa wave). Elliptic shapes represent the total displacement of the sample surface. In case of Sezawa and Rayleigh the depth of the wave decay was found to be two times less for Sezawa than for Rayleigh.
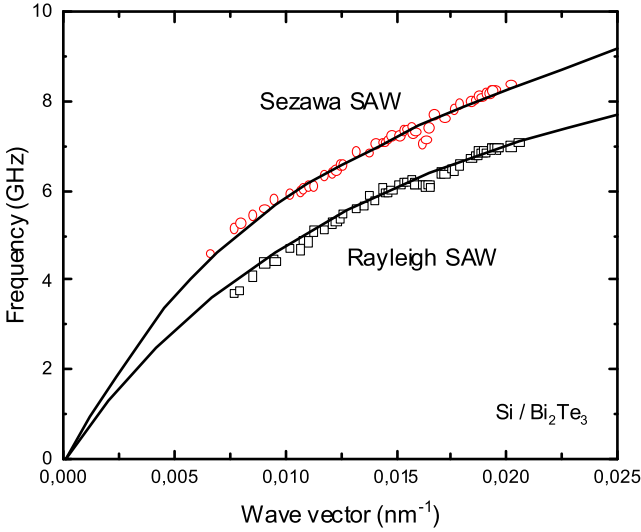
Fig. 3. Dispersion relation and Brillouin spectra for Si/Bi$_2$Te$_3$ heterostructure. (a) Evolution of surface Brillouin spectra of Si/Bi$_2$Te$_3$ heterostructure. (b) Dispersion of surface phonons for Si/Bi$_2$Te$_3$ heterostructure. Both Sezawa (red circles) and Rayleigh (black squares) surface acoustic waves show a small anomaly for $q \approx 0.016$ nm^{-1}. Black lines were obtained from FEM simulations of slow-on-fast system using the known elastic constants of substrate Si and Bi$_2$Te$_3$ [19].

$\upsilon_{SAW} = \frac{\Delta \omega_{SAW} \lambda_0}{2 sin\Theta}$ and $q = \frac{4\pi sin\Theta}{\lambda_0}$, where Θ is the scattering angle (between the incident and normal to the sample), $\Delta \omega_{SAW}$ is the Brillouin frequency shift observed in experiment and $\lambda_0 = 532$ nm in case of our experiment. Such spectrum is presented in Fig. 2.

In order to check whether the experimental dispersion relation shows any anomaly the finite element method (FEM) was use to simulate the phonons frequencies with different wave vectors for the heterostructure as a simple elastic system (slow-on-fast). Simulations were performed using the COMSOL software [27]. In this method the surface wave velocity was determined by the search for the undamped eigenmodes of the 2D unit cell at the periodic boundary conditions. Sezawa and

Rayleigh surface acoustic waves differ in the penetration depth (see insets in Fig. 2) and therefore in the sensitivity to the surface deformation.

The collection of several dozens of spectra allows to plot the dispersion relations for both Sezawa (S) and Raleigh (R) SAW which are presented in Fig. 3. A deep in dispersion relation $\omega(q)$ is visible for both S and R waves at 0.016 nm^{-1}. The relative changes in phonons frequencies are $\Delta \omega / \omega = 0.066$ and 0.047 for S and R respectively. The dip for Sezawa wave is more pronounced, which is obvious when the deformation profiles of both modes are compared (see the insets in Fig. 2). The error bars are of the order of experimental points.

5. Discussion and conclusions

Thalmeier [30] has proposed model which derives the coupling between helical Dirac states and surface phonons by assuming displacement-dependent Dirac cones. Let us follow his approach the continuous long-wavelength deformation of the surface leads to a periodic tilting of the surface normal. Additionally, in the continuum limit without scattering between cones the effect of several cones would simply be additive. The frequency ω_{qs}^2 of surface phonons renormalized by coupling to helical Dirac electrons was obtained from

$$\omega_{qs}^2 = \omega_{qs}^2 \left(\prod^{intra} \left(q, \omega_{qs} \right) + \prod^{inter} (q, \omega_{qs}) \right) \qquad (1)$$

where Π^{intra} and Π^{inter} are the self-energies due to surface electrons of the intra- and interband contributions respectively. Finally, the change of the q-dependent phonon frequency is given by:

$$\Delta_s^0(q) = (\omega_{qs} - \omega_{qs})/\omega_{qs} = \frac{1}{4} \left(\frac{\mu_c}{c_s V_c} \right) \left(\frac{k_c}{k_0} \right)^2 \qquad (2)$$

where: $\omega_q = \upsilon_{SAW} q$ is the frequency, υ_{SAW} the velocity of surface phonon related to elastic constant $c_s = \rho v^2$, $\rho = M/V_c$ is the density and M the atomic mass and V_c volume per atom respectively, $k_0 = \pi/a$ defines the dimension of the Brillouin zone and k_c defines the wave vector where the helical surface states merge with the bulk bands. In the model above the relative change in phonon frequency was calculated for Bi$_2$Se$_3$ to be of the order of 10^{-4}, mainly because of small value of (k_c/k_o) ratio. The limit of the Thalmeier model corresponds to the case of very small phonons wave vectors q $\ll$ k$_F$ = μ/v_F and is limited by wave vector $k_c = \mu_c/v_F$. The anomaly in the surface phonon frequency change depends on the chemical potential or Fermi wave vector. Because of the lack of backscattering the Kohn anomaly appears at $q < 2k_F$. In our case the Kohn anomaly are observed for the wave vectors of the order of 10^{-1} Å^{-1} and are of the same order of magnitude lower than those reported in Ref. 16, 21, 22 and 23. As the Eqs. (1) and (2) are considered the properties of substrate and layer must be used in calculations. The phase velocities of Sezawa (S) and Rayleigh (R) waves can be found from dispersion relation. We found these values to be 2750 m/s and 2300 m/s for S and R waves respectively for the wave vector 0.016 nm^{-1}. The second important factor is k$_0$ = π/a which is approximately at least two times smaller for composite material in comparison to bulk value used in Ref. 31 (29 Å). Using those above-mentioned parameters, we found the relative change in phonon frequency (Eq. (2)) to be 3·10^{-2} and 2·10^{-2} for S and R waves respectively.

Parente et al [31] analyzed the interaction at the surface of a three-dimensional (3D) topological insulator among 2D electron states belonging to the Dirac cone close to the point of the Brillouin zone and the Rayleigh surface phonon mode. They found that the electron–phonon interaction cannot be responsible of strong renormalization effects and they estimate the value of EPC constant λ to be $\sim$ 0.01.

The model basing on separation of intra and interband contributions to the Kohn anomaly was given by Zhu [20]. For the computational purposes the Bi$_2$Se$_3$ bulk sample was transformed into composite system

Rayleigh SAW   Sezawa SAW
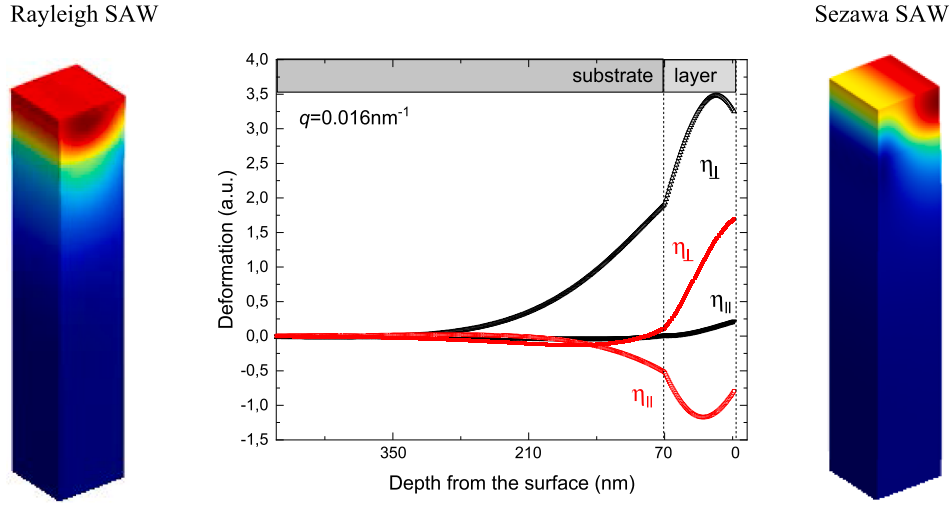
Fig. 4. The relative changes of the surface deformations $\eta_\perp$ and $\eta_{||}$ caused by Rayleigh (black) and Sezawa (red) waves as a function of depth from the sample surface. In the both cases the dominant component is $\eta_\perp$.
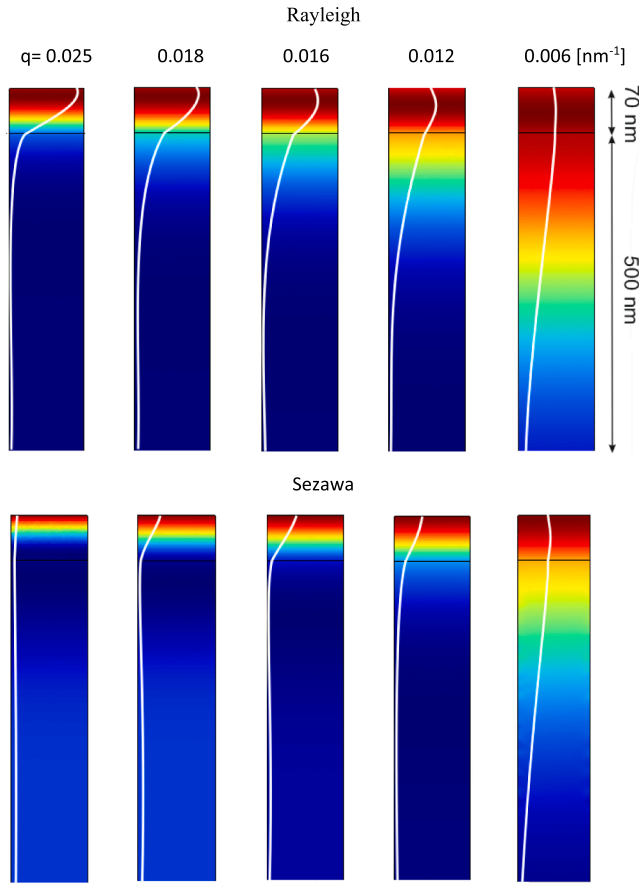
Fig. 5. Deformation fields obtained for Rayleigh and Sezawa waves for different wave vectors in the direction perpendicular to the sample surface. The white lines reflect the deformation profiles for different samples depths (horizontal scale is the same for all wave vectors q).

consisting of an ultrathin metallic film and an underlying insulating substrate. Under assumption of weak dependence of the ionic screened potential V(q) on q and the Thomas-Fermi wave vector $k_F = 0.5$ Å^{-1} they could calculate the coupling constant λ_q. The EPC constant was found to be $\lambda_q = \lambda_\perp + \lambda_{||}$, where $\lambda_\perp$ accounts for the vertical shear component while $\lambda_{||}$ is related to the longitudinal component.

In order to compare our results with those described above we have calculated the deformation profile heterostructure under investigation. Using the FEM it was possible to calculate the relative changes of two deformation component: in plane ($\eta_{||}$) and perpendicular one ($\eta_\perp$) across the unit cell used in simulations. The obtained results are given in the Fig. 4.

The main difference between the two types of phonons is the real depth of the wave decay – the total displacement associated with the propagation of the Sezawa wave is half of the total displacement of the Rayleigh wave. Both exhibit the exponential decay of the wave's amplitude. Due to these features the Sezawa mode has an advantage over the Rayleigh one when studying the electron–phonon coupling. Small penetration depth reduced the bulk coupling to electrons and the high sensitivity to the deformation reflected the dependency between the surface deformation and the surface states of the sample (displacement-dependent Dirac cones).

The observed behavior is in agreement with classical approach to the surface waves depth dependence [29]. The only difference is the discontinuity observed at the semiconductor- topological insulator interface, which is the border of slow-on-fast heterostructure. Zhu [17] found that $\lambda_{||}/\lambda_\perp = 0.65$ best represents the observed Kohn anomaly as detected in their HASS experiment. In case of experiment presented this ratio was found to be 0.4 at the sample surface. Heading towards lower energies it is worth to notice that in Thalmeier model [30] tested for ultrasonic frequencies (MHz) the $\lambda_{||}$ has been set to be 0 without prejudice to the transparency of the model.

So far reported values for the electron–phonon coupling constant λ varied greatly even for the same compound. For Bi$_2$Se$_3$, various ARPES studies gave values ranging from 10^{-2} up to 10^1 [32-36]. Similarly, the values of λ obtained from theoretical calculation are inconsistent and cover two orders of magnitude [37,38].

For a thin film/substrate heterostructure, there are two sources of electron phonon interaction - the surface and the interface. The deformation potential of surface phonons determines their capability for an investigation of the EPC along z-direction of the heterostructure. In order to determine exactly from which part of sample Brillouin spectroscopy gives reliable information, FEM simulations were performed for different wave vectors for both Sezawa and Rayleigh waves (see Fig. 5).

Large deformation potential of a surface phonons implies large penetration depth. Both, the Rayleigh and Sezawa phonons, differ in their penetration depth. The penetration depth of the Rayleigh phonon is larger when comparing to the Sezawa mode. As a result, their interaction with electrons differs. Phonons can couple to electrons at the

Fermi surface (the Kohn effect) as well as below the surface, as recently reported from ARPES experiments ref. [39].

To determine an origin of the electron–phonon interaction in the Si/Bi$_2$Te$_3$ heterostructure we have to refer to our previous experiments related with the EPC in the GaAs/Bi$_2$Te$_3$ heterostructure [7]. Reported here anomalies of the surface phonons dispersions of Rayleigh and Sezawa modes were observed at $E_{R\_GaAs} = 3.2$ GHz ($1.30 \cdot 10^{-2}$ meV) for $q_{R\_GaAs} = 0.012$ nm^{-1} and $E_{S\_GaAs} = 5$ GHz ($2.1 \cdot 10^{-2}$ meV) and $q_{S\_GaAs} = 0.010$ nm^{-1} respectively (see Fig. 2 in [7]). Its origin was ascribed to the EPC at the interface between the topological insulator and the substrate, because only electrons localized at the interface revealed a Hall mobility. Calculated correction of the phonon frequency of the heterostructure [7] was linearly dependent on the Fermi energy. Additionally, the density functional theory (DFT) calculations revealed an emergence of the Dirac cone at the interface between the topological insulator and GaAs substrate. Analyzed in this paper dispersion relation of the Si/Bi$_2$Te$_3$ heterostructure revealed a small but clearly visible (outside the range of measurement accuracy) anomalies of both Sezawa and Rayleigh waves $E_{S\_Si} = 6.8$ GHz ($2.8\ 10^{-2}$ meV) and $E_{R\_Si} = 6.0$ GHz ($2.5\ 10^{-2}$ meV) at $q = 0.016$ nm^{-1}.

In order to determine exactly from which part of sample Brillouin spectroscopy gives reliable information, FEM simulations were performed for different wave vectors for both Sezawa and Rayleigh waves (see Fig. 5). Reported for both heterostructures anomalies in dispersion relations differ. It may result from physical properties of substrates applied in both heterostructures. According to the mentioned above formula, the correction to the phonon frequency depends on the Fermi energy. Work functions W of a GaAs and Si substrates are 4.77 eV and 4.6 eV, respectively. As a result, the Fermi level of the GaAs/TI sample was lower when comparing to the Fermi level of the Si/TI system. The linear energy dispersion of the Dirac cone implies that the ratio of E/q should be similar for phonons coupled to electrons in the cone for both investigated samples. Only Sezawa phonons fulfilled the condition $\frac{E_{S\_GaAs}}{q_{S\_GaAs}} \approx \frac{E_{S_{Si}}}{q_{S_{Si}}}$ suggesting coupling to electrons in the Dirac cone. Due to the fact that Rayleigh phonons penetrated the substrates (in both heterostructures), their softening can be rather related with coupling to electrons located at other states, where the linear dispersion relation E(q) is not fulfilled. Unfortunately, from these experiments it is not possible to determine to which exactly electrons they coupled.

We believe that the best evidence of electron–phonon coupling is direct experimental observation. Surface dynamics can be probed by means of helium atoms surface scattering (HASS) or surface Brillouin scattering, which was used in studies presented and according to [40] helium scattering takes place just above the sample's surface. This means that, it is not the total electron density of the substrate surface which matters and determines the interaction but the electronic wave functions close to the Fermi level. In other words, the He atom couples directly to surface states of the sample which are the result of electrons excitations.

The energy range offered by Brillouin scattering technique cannot rather be considered as an advantage over helium atoms scattering however it gives a possibility to observe surface excitations (close to the Γ point of the Brillouin zone) which are not accessible for HASS. In addition, an important feature of surface Brillouin spectroscopy of the substrate-thin film system are two simultaneous material responses but coming from different sample depths defined by Sezawa and Rayleigh waves deformation profiles. It is obvious that due to a small momentum range of the Dirac cone only long-wavelength acoustic phonons can participate in the EPC but their energies are very small. Such behavior was confirmed in our experiments for the two heterostructures: thin films of topological insulator Bi$_2$Te$_3$ grown on semiconducting substrates GaAs [7] and Si. This result, for the first time, indicate the possibility of appearance of EPC in such a low energy range (10^{-2} meV) which is lower of two or three orders of magnitude in comparison to those observed in helium atom surface, neutron or inelastic x-ray

scattering [20,21] however in the same range of wave vector (0.1 and 0.16 Å^{-1}).

Finally, when the potential application of topological insulators is considered the large bulk gap of Bi$_2$Te$_3$ points to promising potential for high-temperature spintronics applications [41,42] however it may be hindered by limited lifetimes due to intrinsic many-body interactions, in particular electron–phonon coupling. Nevertheless, we hope that our results will trigger an interest for new research, both experimental and theoretical.

Declaration of Competing Interest

The authors declare that they have no known competing financial interests or personal relationships that could have appeared to influence the work reported in this paper.

References

[1] Zhaoyang Lin, Yu Huang, Xiangfeng Duan, Van der Waals thin-film electronics, Nat. Electron. 2 (2019) 378, https://doi.org/10.1038/s41928-019-0301-7.

[2] E. Pop, Energy dissipation and transport in nanoscale devices, Nano Res. 3 (2010) 147–169, https://doi.org/10.1007/s12274-010-1019-z.

[3] M. Nomura, J. Shiomi, T. Shiga, R. Anufriev, Thermal phonon engineering by tailored nanostructures, Jap. J. Appl. Phys. 57 (2018), 080101, https://doi.org/10.7567/JJAP.57.080101.

[4] J.M. Ziman, Electrons and Phonons: The Theory of Transport Phenomena in Solids, Oxford University Press, New York, 2001, p. 463.

[5] W. Kohn, Images of the Fermi surface in phonon spectra of metals, Phys. Rev. Lett. 2 (1959) 393, https://doi.org/10.1103/PhysRevLett.2.393.

[6] Fang Liu, Wenjing Wu, Yusong Bai, Sang Hoon Chae, Qiuyang Li, Jue Wang, James Hone, X.-Y. Zhu, Disassembling 2D van der Waals crystals into macroscopic monolayers and reassembling into artificial lattices, Science 367 (2020) 903. DOI: 10.1126/science.aba1416.

[7] M. Wiesner, et al., The electron phonon interaction at deep Bi$_2$Te$_3$-semiconductor interfaces from Brillouin light scattering, Sci. Rep. 7 (2017) 16449, https://doi.org/10.1038/s41598-017-16313-5.

[8] L.L. Li, W. Xu, Absorption of surface acoustic waves by topological insulator thin films, Appl. Phys. Lett. 105 (2014), 063503, https://doi.org/10.1063/1.4893002.

[9] H. Zhang, et al., Topological insulators in Bi$_2$Se$_3$, Bi$_2$Te$_3$ and Sb$_2$Te$_3$ with a single Dirac cone on the surface, Nat. Phys. 5 (2009) 438–442, https://doi.org/10.1038/nphys1270.

[10] Z.-G. Chen, G.F. Han, L. Yang, L. Cheng, J. Zou, Nanostructured thermoelectric materials: current research and future challenge, Prog. Nat. Sci. Mater. Int. 22 (2012) 535–549s, https://doi.org/10.1016/j.pnsc.2012.11.011.

[11] O. Caha, et al., Growth, structure, and electronic properties of epitaxial bismuth telluride topological insulator films on BaF2 (111) substrates, Cryst. Grown Des. 13 (2013) 3365–3373, https://doi.org/10.1021/cg400048g.

[12] N. Fuschillo, R. Gibson, Solar Thermoelectric Generators for Missions Toward the Sun, IEEE Trans. Aerosp. Electron. Syst. AES-2 (1966) 93–102, https://doi.org/10.1109/TAES.1966.4501828.

[13] A.F. Gibson, T.S. Moss, The photoconductivity of Bismuth sulphide and bismuth telluride, Proc. Phys. Soc. London, Sect. A 63 (2) (1950) 176, https://doi.org/10.1088/0370-1298/63/2/112.

[14] C.B. Satterthwaite, R. Ure, Electrical and thermal properties of Bi2Te3, Phys. Rev. 108 (5) (1957) 1164, https://doi.org/10.1103/PhysRev.108.1164.

[15] Y.C. Akgös, G.A. Saunders, Z. Sümengen, Elastic wave propagation in Bi$_{1.60}$Sb$_{0.40}$Te$_3$ and Bi$_2$Te$_3$, J. Mater. Sci. 7 (1972) 279–288.

[16] J.O. Jenkins, J.A. Rayne, R.W. Jr, Ure, Elastic moduli and phonon properties of Bi$_2$Te$_3$, Erratum Phys. Rev. B 6, (1972) 1609, Phys. Rev. B 5 (1972) 3171, https://doi.org/10.1103/PhysRevB.5.3171 10.1103/PhysRevB.6.1609.5.

[17] C. Lamuta, et al., Mechanical properties of Bi$_2$Te$_3$ topological insulator investigated by density functional theory and nanoindentation, Scr. Mater. 121 (2016) 50–55, https://doi.org/10.1016/j.scriptamat.2016.04.036.

[18] A. Trzaskowska, B. Mroz, Surface phonons in topological insulator Bi2Te3 investigated by Brillouin light scattering, Sci. Rep. 10 (2020) 11812, https://doi.org/10.1038/s41598-020-68690-z.

[19] G. Wang, et al., Topological insulator thin films of Bi$_2$Te$_3$ with controlled electronic structure, Adv. Mater. 23 (2011) 2929–2932, https://doi.org/10.1002/adma.201100678.

[20] X. Zhu, et al., Interaction of phonons and dirac fermions on the surface of Bi$_2$Se$_3$: A Strong Kohn Anomaly, PRL 107 (2011), 186102, https://doi.org/10.1103/PhysRevLett.107.186102.

[21] F. Weber, et al., Extended phonon collapse and the origin of the charge-density wave in 2H−NbSe$_2$, PRL 107 (2011), 107403, https://doi.org/10.1103/PhysRevLett.107.107403.

[22] R. Mook, C.R. Watson Jr, Neutron Inelastic Scattering Study of Tetrathiafulvalene Tetracyanoquinodimethane (TTF-TCNQ), PRL 36 (1976) 801, https://doi.org/10.1103/PhysRevLett.36.801.

[23] A. Fülöp, et al., Phase transition of bismuth telluride thin films grown by MBE, Appl. Phys. Express 7 (2014), 045503, https://doi.org/10.7567/APEX.7.045503.

[24] F. Scarponi, et al., High-performance versatile setup for simultaneous Brillouin-Raman Microspectroscopy, Phys. Rev. X 7 (2017), 031015, https://doi.org/10.1103/PhysRevX.7.031015.

[25] S.M. Lindsay, M.W. Anderson, J.R. Sandercock, Construction and alignment of a high performance multipass vernier tandem Fabry-Perot interferometer, Rev. Sci. Instrum. 52 (10) (1981) 1478–1486, https://doi.org/10.1063/1.1136479.

[26] J.G. Dil, N.C.J.A. van Hijningen, F. van Dorst, R.M. Aarts, Tandem multipass Fabry-Perot interferometer for Brillouin scattering, Appl. Opt. 20 (8) (1981) 1374–1381, https://doi.org/10.1364/AO.20.001374.

[27] COMSOL Multiphysics finite element software, COMSOL AB, Sweden.

[28] P. Gómez García, J.-P. Fernández-Álvarez, Floquet-Bloch theory and its application to the dispersion curves of nonperiodic layered systems, Math. Probl. Eng. 2015 (2015), 475364, https://doi.org/10.1155/2015/475364.

[29] G.W. Farnell, L. Adler, Elastic wave propagation in thin layers, Phys. Acoust. 9 (1972) 35–127, https://doi.org/10.1016/B978-0-12-395670-5.50007-6.

[30] P. Thalmeier, Surface phonon propagation in topological insulators, Phys. Rev. B 83 (2011), 125314, https://doi.org/10.1103/PhysRevB.83.125314.

[31] V. Parente, A. Tagliacozzo, F. von Oppen, F. Guinea, Electron-phonon interaction on the surface of a three-dimensional topological insulator, Phys. Rev. B 88 (2013), 075432, https://doi.org/10.1103/PhysRevB.88.075432.

[32] C. Chen, et al., Experimental realization of a three-dimensional topological insulator, Bi$_2$Te$_3$ Science 325 (2009) 178–181, https://doi.org/10.1126/science.1173034.

[33] S.R. Park, et al., Quasiparticle scattering and the protected nature of the topological states in a parent topological insulator Bi$_2$Se$_3$, Phys. Rev. B 81 (2010), 041405, https://doi.org/10.1103/PhysRevB.81.041405.

[34] R.C. Hatch, et al., Stability of the Bi$_2$Se$_3$(111) topological state: Electron-phonon and electron-defect scattering, Phys. Rev. B 83 (2011), 241303, https://doi.org/10.1103/PhysRevB.83.241303.

[35] T. Kondo, et al., Anomalous dressing of Dirac fermions in the topological surface state of Bi$_2$Se$_3$, Bi$_2$Te$_3$ and Cu-doped Bi$_2$Se$_3$, PRL 110 (2013), 217601, https://doi.org/10.1103/PhysRevLett.110.217601.

[36] Z.-H. Pan, A.V. Fedorov, D. Gardner, Y.S. Lee, S. Chu, T. Valla, Measurement of an exceptionally weak electron-phonon coupling on the surface of the topological insulator Bi$_2$Se$_3$ using angle-resolved photoemission spectroscopy, PRL 108 (2012), 187001, https://doi.org/10.1103/PhysRevLett.108.187001.

[37] S. Giraud, A. Kundu, R. Egger, Electron-phonon scattering in topological insulator thin films, Phys. Rev. B 85 (2012), 035441, https://doi.org/10.1103/PhysRevB.85.035441.

[38] V. Parente, A. Tagliacozzovon, F. Oppen, F. Guinea, Electron-phonon interaction on the surface of a three-dimensional topological insulator, Phys. Rev. B 88 (2013) 075432 ttps://doi.org/10.1103/PhysRevB.88.075432.

[39] Xiao-Fang Tang, Yu-Xia Duan, Fan-Ying Wu, Shu-Yu Liu, Chen Zhang, Yin-Zou Zhao, Jiao-Jiao Song, Yang Luo, Qi-Yi Wu, Jun He, H. Y. Liu, Wen Xu, Jian-Qiao Meng, Three-dimensional Fermi surface and electron-phonon coupling in semimetallic 1T- TiTe2 studied by angle-resolved photoemission spectroscopy, Phys. Rev. B 99 (2019) 125112. doi.org/10.1103/PhysRevB.99.125112.

[40] B. Kohler, P. Ruggerone, M. Scheffler, *Ab initio* study of the anomalies in the He-atom-scattering spectra of H/Mo(110) and H/W(110), Phys. Rev. B 56 (1997) 13503, https://doi.org/10.1103/PhysRevB.56.13503.

[41] J. Moore, Topological insulators the next generation, Nat. Phys. 5 (2009) 378–380, https://doi.org/10.1038/nphys1294.

[42] A. Dyrdal, J. Barnas, A. Fert, Spin-Momentum-Locking Inhomogeneities as a Source of Bilinear Magnetoresistance in Topological Insulators, PRL 124 (2020), 046802, https://doi.org/10.1103/PhysRevLett.124.046802.